axis whereas in the $(20\bar{1})$ plane of the bromanil salt the donor and acceptor stacks are tilted in opposite directions to each other. In addition, there is a slight difference in the relative arrangements of the stacks in the direction normal to the $(20\bar{1})$ plane of the bromanil salt compared to the arrangement perpendicular to the $(10\bar{1})$ plane of the TCNQ salt. This difference can also be seen by comparison of Figs. 1(*b*) and 2(*b*).

Conclusion

In this paper we have reported the structure of the first 1:1 organic charge-transfer salt to exhibit segregated stacking of donors and acceptors that does not contain TCNQ or a TCNQ-like molecule. The striking similarity that the structure of TMTTF–brl bears to that of TMTTF–TCNQ (Phillips *et al.*, 1976) has been demonstrated. The most noteworthy difference between the two structures is the difference in the interplanar spacing of the acceptor molecules. The 0·1 Å larger spacing in TMTTF–brl is probably caused by the bulk of the Br atoms. A similar effect occurs in the dibenzotetrathiafulvalene (DBTTF) salt of $TCNQCl_2$, in which the 3·41 Å spacing (Soling, Rindorf & Thorup, 1981) between acceptor molecules is presumably caused by the bulk of the Cl atoms. The resultant weakening of the intermolecular π overlap in the acceptor stacks of these materials is probably related to the appreciably lower conductivity of TMTTF–brl and DBTTF–$TCNQCl_2$ (Jacobsen, Pedersen, Mortensen & Bechgaard, 1980) compared to that of TMTTF–TCNQ.

References

BERLINSKY, A. J., CAROLAN, J. F. & WEILER, L. (1976). *Solid State Commun.* **19**, 1165–1168.

CARRUTHERS, T., BLOCH, A. N. & COWAN, D. O. (1976). *Bull. Am. Phys. Soc.* **21**, 213.

CROWLEY, J. I. (1980). Private communication.

International Tables for X-ray Crystallography (1974). Vol. IV. Birmingham: Kynoch Press.

JACOBSEN, C. S., PEDERSEN, H. J., MORTENSEN, K. & BECHGAARD, K. (1980). *J. Phys. C.* **13**, 3411–3425.

MAYERLE, J. J. (1977). *Inorg. Chem.* **16**, 916–919.

MAYERLE, J. J. (1980). *Mixed-Valence Compounds*, edited by D. B. BROWN, pp. 451–473. Dordrecht: Reidel.

MAYERLE, J. J. & TORRANCE, J. B. (1980*a*). *Bull. Chem. Soc. Jpn.* Submitted.

MAYERLE, J. J. & TORRANCE, J. B. (1980*b*). Unpublished results.

MAYERLE, J. J., TORRANCE, J. B. & CROWLEY, J. I. (1979). *Acta Cryst.* B**35**, 2988–2995.

METZGER, R. M. (1978). Private communication.

PAULING, L. (1960). *The Nature of the Chemical Bond*, 3rd ed., p. 260. Ithaca: Cornell Univ. Press.

PHILLIPS, T. E., KISTENMACHER, T. J., BLOCH, A. N., FERRARIS, J. P. & COWAN, D. O. (1976). *Acta Cryst.* B**33**, 422–428.

SOLING, H., RINDORF, G. & THORUP, N. (1981). *Acta Cryst.* B**37**, 1716–1719.

TORRANCE, J. B. (1979). *Acc. Chem. Res.* **12**, 79–86.

TORRANCE, J. B., MAYERLE, J. J., LEE, V. Y. & BECHGAARD, K. (1979). *J. Am. Chem. Soc.* **101**, 4747–4748.

TORRANCE, J. B., MAYERLE, J. J., LEE, V. Y., BOZIO, R. & PECILE, C. (1981). *Solid State Commun.* Submitted.

Acta Cryst. (1981). B**37**, 2034–2043

The Structures of *N*-(*n*-Propyl)pyridinium–7,7,8,8-Tetracyano-*p*-quinodimethane (1:2) [$NPPy^+.(TCNQ)_2^-$] and *N*-(*n*-Butyl)pyridinium–7,7,8,8-Tetracyano-*p*-quinodimethane (4:7) [$(NBPy^+)_4.(TCNQ)_7^{4-}$]

BY M. KONNO AND Y. SAITO*

The Institute for Solid State Physics, The University of Tokyo, Roppongi-7, Minato-ku, Tokyo 106, *Japan*

(*Received* 13 *November* 1980; *accepted* 6 *April* 1981)

Abstract

The crystal structures of $NPPy^+.(TCNQ)_2^-$ and $(NBPy^+)_4.(TCNQ)_7^{4-}$ have been determined at 297 K by X-ray diffraction. Crystals of the former are triclinic with space group $P\bar{1}$, a = 14·5419 (19), b = 13·7233 (14), c = 7·8016 (9) Å, α = 104·059 (10), β = 110·723 (12), γ = 94·084 (11)°, V = 1391·2 (2) Å^3 and Z = 2. Those of the latter are triclinic with space group $P\bar{1}$, a = 15·0448 (10), b = 17·3667 (14), c = 10·4666 (9) Å, α = 105·557 (7), β = 98·007 (7), γ = 96·913 (6)°, V = 2572·9 (3) Å^3 and Z = 1. Refine-

* Present address: Department of Chemistry, Faculty of Science and Engineering, Keio University, 3-14-1 Hiyoshi, Kohoku-ku, Yokohama 223, Japan.

0567-7408/81/112034-10$01.00

ments by the block-diagonal least-squares method reduced the respective R values to 0·051 and 0·053 for 3529 and 5033 independent reflections. Crystals of $NPPY^+.(TCNQ)_2^-$ undergo a first-order phase transition from insulator to metal at about 388 K. In the low-temperature phase, TCNQ anions are stacked plane-to-plane along **a**. The four TCNQ anions per unit cell form two crystallographically independent dimers with interplanar spacings of 3·234 and 3·185 Å, whereas, above the transition temperature, X-ray evidence suggests that the TCNQ anions stack uniformly in a zigzag way and the $NPPy^+$ cations exhibit rotational disorder. In $(NBPy^+)_4.(TCNQ)_7^{4-}$, TCNQ anions are stacked plane-to-plane along [102] and form a heptamer with interplanar spacings of 3·220, 3·329 and 3·363 Å. The butyl groups of two crystallographically independent $NBPy^+$ cations exhibit orientational disorder.

Introduction

Quasi-one-dimensional tetracyano-*p*-quinodimethane (TCNQ) radical salts have been extensively studied with a great deal of interest because of the variety of their electronic and magnetic properties and the phase transition due to the instability for lattice distortion in the one-dimensional uniform linear chain. Alkali-metal TCNQ salts (except Li) undergo an insulator–insulator (*I–I*) transition with dimerization in the uniform linear chain (Vegter, Himba & Kommandeur, 1969; Kommandeur, 1975; Konno & Saito, 1975; Konno, Ishii & Saito, 1977). This transition has been interpreted as follows: in the system of the one-dimensional antiferromagnetic Heisenberg chain there is instability for the lattice distortion of wavevector $2\mathbf{k}_F$ and the spin Peierls transition occurs at low temperature, where $\mathbf{k}_F$ is the one-electron Fermi wavevector (Beni & Pincus, 1972; Pytte, 1974; Jacobs, Bray, Hart, Interrante, Kasper, Watkins, Prober & Bonner, 1976; Torrance, 1978). On the other hand, an *I–I* transition was also observed in methyltriphenylphosphonium–$(TCNQ)_2$ (Kepler, 1963), but this change was revealed as the rotation of the phenyl group of the cation with breaking of the hydrogen bonds between cations and anions (Konno & Saito, 1973). The most prominent tetrathiafulvalene compound (TTF–TCNQ), which has been paid particular attention because of its high electrical conductivity, undergoes a metal–insulator (*M–I*) transition with two kinds of lattice distortions of wavevectors at $2\mathbf{k}_F$ and $4\mathbf{k}_F$. Several models have been proposed concerning the origin of this transition (Emery, 1976; Torrance, 1977; Sumi, 1977; Fletcher & Toombs, 1977). It was found that in *N*-ethyl-*N*-methylmorpholinium(MEM)–$(TCNQ)_2$ an electronic Peierls transition takes place for wavevector $4\mathbf{k}_F$ $[= \rho(2\pi)/b]$ at about 335 K and a spin Peierls transition for $2\mathbf{k}_F$ $[= \rho/2(2\pi)/b]$ at about 20 K since this system is a spinless fermion, where b is the spacing between the molecules along the stack and ρ is the electron density per lattice site (Huizinga, Kommandeur, Sawatzky, Thole, Kopinga, de Jonge & Roos, 1979). Yoshimura & Murakami (1978) and Murakami & Yoshimura (1980) reported that $NPPy$–$(TCNQ)_2$ exhibits a first-order *M–I* transition while $(NBPy)_4$–$(TCNQ)_7$ undergoes a first-order *I–I* transition. In the latter case, electrical conductivity reduces above the transition temperature in contrast to other examples described above. We determined the crystal structures of both TCNQ salts in order to elucidate these transitions from the structural point of view.

Experimental

Crystals were kindly supplied by M. Murakami of Matsushita Research Institute Tokyo, Inc. Preliminary oscillation and Weissenberg photographs showed both

Table 1. *Additional crystal data and experimental conditions for* $NPPy^+.(TCNQ)_2^-$ *and* $(NBPy^+)_4.(TCNQ)_7^{4-}$ *at* 297 K

	$NPPy^+.(TCNQ)_2^-$	$(NBPy^+)_4.(TCNQ)_7^{4-}$
Formula	$C_8H_{12}N^+.(C_{12}H_4N_4)_2^-$	$(C_9H_{14}N^+)_4.(C_{12}H_4N_4)_7^{4-}$
M_r	530·6	1974·2
D_m (Mg m^{-3})	1·268	1·274
D_x (Mg m^{-3})	1·267	1·274
μ(Mo $K\alpha$) (mm^{-1})	0·087	0·087
Crystal dimensions (mm)	0·17 × 0·30 × 0·25	0·20 × 0·32 × 0·27
Radiation	Mo $K\alpha$ (λ = 0·71069 Å)	Mo $K\alpha$ (λ = 0·71069 Å)
Monochromator	Graphite plate	Graphite plate
Scanning mode	ω–2θ	ω–2θ
$\Delta\omega$ (°)	0·9 + 0·7 tan θ	0·8 + 0·8 tan θ
Maximum 2θ (°)	55	50
Number of independent reflections $[\lvert F_o\rvert > 3\sigma(\lvert F_o\rvert)]$	3529	5033
$R = \sum \lvert\lvert F_o\rvert - \lvert F_c\rvert\rvert / \sum \lvert F_o\rvert$	0·051	0·053
$R_2 = [\sum (\lvert F_o\rvert - \lvert F_c\rvert)^2 / \sum \lvert F_o\rvert^2]^{1/2}$	0·048	0·050

crystals to be triclinic. The space group was later confirmed to be $P\bar{1}$ rather than $P1$ by the structure refinements. The unit-cell dimensions were refined by the least-squares method based on the θ values of 25 reflections for NPPy$^+$.(TCNQ)$_2^-$ and of 36 reflections for (NBPy$^+$)$_4$.(TCNQ)$_7^{4-}$. The experimental density measurements (flotation method; benzene–carbon tetrachloride) revealed that NPPy and NBPy radical salts have exact composition ratios of 1:2 and 4:7 respectively. Crystal data and experimental conditions are summarized in the *Abstract* and Table 1. Intensity data were collected on an automated four-circle diffractometer. Lorentz and polarization corrections were applied but no correction for absorption was made.

Structure determination

Both structures were solved in a similar fashion. Positions of TCNQ moieties were deduced from sharpened Patterson maps. Successive three-dimensional electron-density syntheses phased with the TCNQ moieties revealed the positions of the pyridine rings. After several cycles of refinement it was found that the butyl groups of two crystallographically independent NBPy$^+$ cations in (NBPy$^+$)$_4$.(TCNQ)$_7^{4-}$ exhibit orientational disorder. Positions of all the H atoms were deduced from a difference synthesis. The block-diagonal least-squares program *HBLS*-4 (T. Ashida) was employed using anisotropic thermal parameters for non-hydrogen atoms and isotropic for H. The atomic scattering factors for non-hydrogen atoms were taken from *International Tables for X-ray Crystallography* (1974) and for H from Stewart, Davidson & Simpson (1965). Unit weight was adopted for all the reflections. The R values reduced to 0·056 for NPPy$^+$.(TCNQ)$_2^-$ and to 0·075 for (NBPy$^+$)$_4$.(TCNQ)$_7^{4-}$. At this stage, three reflections of the former and four of the latter with the largest $|F_c|$ values, which were apparently affected by extinction, were excluded from the refinements. Several further refinements gave $R = 0{\cdot}051$ for NPPy$^+$.(TCNQ)$_2^-$ and $R = 0{\cdot}053$ for (NBPy$^+$)$_4$.(TCNQ)$_7^{4-}$. At the final stage of the refinement all the shifts were less than one tenth of the corresponding standard deviations. Final atomic parameters are given in Table 2.*

Table 2. *Positional parameters* ($\times 10^4$, *for* H $\times 10^3$) *and isotropic thermal parameters* (Å^2 $\times 10^2$) *with e.s.d.'s in parentheses*

For non-hydrogen atoms $B_{eq} = \frac{8}{3}\pi^2 \sum_i \sum_j U_{ij}\, a_i^* a_j^* \mathbf{a}_i.\mathbf{a}_j$.

NPPy$^+$.(TCNQ)$_2^-$

	x	y	z	B_{eq}/B
C(*A*1)	821 (2)	−810 (2)	346 (4)	34 (1)
C(*A*2)	1393 (2)	71 (2)	303 (4)	35 (1)
C(*A*3)	1794 (2)	896 (2)	1847 (4)	36 (1)
C(*A*4)	1682 (2)	921 (2)	3604 (4)	34 (1)
C(*A*5)	1117 (2)	31 (2)	3650 (4)	37 (1)
C(*A*6)	706 (2)	−786 (2)	2105 (4)	38 (1)
C(*A*7)	396 (2)	−1652 (2)	−1248 (4)	37 (1)
C(*A*8)	2103 (2)	1762 (2)	5212 (4)	36 (1)
C(*A*9)	−193 (2)	−2527 (2)	−1234 (4)	44 (1)
C(*A*10)	512 (2)	−1706 (2)	−3005 (4)	41 (1)
C(*A*11)	2648 (2)	2666 (2)	5202 (4)	42 (1)
C(*A*12)	2026 (2)	1779 (2)	6987 (4)	41 (1)
N(*A*1)	−678 (2)	−3218 (2)	−1240 (4)	63 (1)
N(*A*2)	598 (2)	−1749 (2)	−4420 (4)	57 (1)
N(*A*3)	3074 (2)	3400 (2)	5220 (4)	61 (1)
N(*A*4)	1982 (2)	1805 (2)	8424 (4)	59 (1)
C(*B*1)	3221 (2)	−1367 (2)	−2977 (4)	36 (1)
C(*B*2)	3516 (2)	−417 (2)	−3251 (4)	38 (1)
C(*B*3)	3888 (2)	448 (2)	−1771 (4)	38 (1)
C(*B*4)	4003 (2)	448 (2)	131 (4)	35 (1)
C(*B*5)	3728 (2)	−511 (2)	403 (4)	38 (1)
C(*B*6)	3350 (2)	−1370 (2)	−1078 (4)	38 (1)
C(*B*7)	2814 (2)	−2253 (2)	−4492 (4)	40 (1)
C(*B*8)	4356 (2)	1335 (2)	1642 (4)	38 (1)
C(*B*9)	2515 (2)	−3182 (2)	−4183 (4)	45 (1)
C(*B*10)	2665 (2)	−2292 (2)	−6418 (4)	47 (1)
C(*B*11)	4589 (2)	2312 (2)	1415 (4)	46 (1)
C(*B*12)	4475 (2)	1333 (2)	3544 (4)	43 (1)
N(*B*1)	2297 (2)	−3930 (2)	−3906 (4)	60 (1)
N(*B*2)	2552 (2)	−2333 (2)	−7955 (4)	65 (1)
N(*B*3)	4772 (3)	3103 (2)	1271 (4)	70 (1)
N(*B*4)	4568 (2)	1339 (2)	5062 (4)	60 (1)
N(*P*1)	2810 (2)	4899 (2)	397 (4)	47 (1)
C(*P*1)	3523 (3)	5471 (3)	151 (5)	58 (1)
C(*P*2)	4369 (3)	5972 (3)	1666 (6)	64 (2)
C(*P*3)	4505 (2)	5912 (3)	3472 (5)	57 (1)
C(*P*4)	3774 (2)	5326 (3)	3691 (5)	52 (1)
C(*P*5)	2939 (2)	4826 (2)	2154 (5)	49 (1)
C(*P*6)	1854 (3)	4399 (2)	−1232 (5)	58 (1)
C(*P*7)	1044 (3)	5014 (3)	−1325 (5)	55 (1)
C(*P*8)	63 (3)	4445 (3)	−2923 (6)	79 (2)
H(*A*2)	147 (2)	6 (2)	−90 (3)	34 (5)
H(*A*3)	215 (2)	148 (2)	180 (3)	30 (5)
H(*A*5)	104 (2)	7 (2)	483 (3)	35 (5)
H(*A*6)	35 (2)	−136 (2)	218 (3)	43 (6)
H(*B*2)	342 (2)	−42 (2)	−453 (3)	37 (5)
H(*B*3)	408 (2)	110 (2)	−197 (3)	37 (5)
H(*B*5)	379 (2)	−52 (2)	164 (3)	31 (5)
H(*B*6)	317 (2)	−200 (2)	−85 (3)	42 (6)
H(*P*1)	335 (2)	543 (2)	−120 (4)	62 (7)
H(*P*2)	491 (2)	640 (2)	153 (4)	75 (8)
H(*P*3)	511 (2)	633 (2)	465 (4)	73 (8)
H(*P*4)	383 (2)	527 (2)	498 (4)	57 (7)
H(*P*5)	238 (2)	440 (2)	215 (4)	59 (7)
H(*P*6*a*)	204 (2)	427 (2)	−238 (4)	58 (7)
H(*P*6*b*)	172 (2)	372 (2)	−113 (4)	59 (7)
H(*P*7*a*)	123 (2)	571 (2)	−145 (4)	61 (7)
H(*P*7*b*)	96 (2)	519 (2)	−4 (4)	59 (7)
H(*P*8*a*)	21 (2)	417 (2)	−415 (5)	85 (9)
H(*P*8*b*)	−51 (3)	490 (3)	−308 (5)	100 (10)
H(*P*8*c*)	−14 (2)	378 (2)	−267 (5)	84 (9)

* Lists of structure factors and anisotropic thermal parameters for both compounds have been deposited with the British Library Lending Division as Supplementary Publication No. SUP 36149 (61 pp.). Copies may be obtained through The Executive Secretary, International Union of Crystallography, 5 Abbey Square, Chester CH1 2HU, England.

Table 2 (*cont.*)

$(NBPy^+)_4.(TCNQ)_7^{4-}$

	x	y	z	B_{eq}/B		x	y	z	B_{eq}/B
C(*A*1)	239 (2)	3041 (2)	2562 (3)	31 (1)	C(*P*6)	1817 (3)	5673 (2)	−584 (4)	55 (1)
C(*A*2)	930 (2)	2764 (2)	1834 (3)	33 (1)	C(*P*7)	2613 (3)	5555 (2)	338 (4)	46 (1)
C(*A*3)	1048 (2)	1982 (2)	1529 (3)	32 (1)	C(*P*8*a*)†	2857 (3)	4720 (3)	−234 (5)	39 (2)
C(*A*4)	488 (2)	1395 (2)	1933 (3)	29 (1)	C(*P*8*b*)†	3138 (15)	4797 (13)	−608 (30)	52 (9)
C(*A*5)	−206 (2)	1667 (2)	2643 (3)	31 (1)	C(*P*8*c*)†	2484 (15)	4580 (16)	−176 (32)	51 (10)
C(*A*6)	−323 (2)	2454 (2)	2954 (3)	31 (1)	C(*P*9*a*)†	3643 (4)	4554 (4)	686 (8)	40 (2)
C(*A*7)	97 (2)	3848 (2)	2836 (3)	33 (1)	C(*P*9*b*)†	3971 (9)	4769 (9)	487 (16)	44 (5)
C(*A*8)	626 (2)	588 (2)	1644 (3)	29 (1)	C(*P*9*c*)†	3357 (8)	4411 (9)	944 (16)	39 (5)
C(*A*9)	−594 (3)	4135 (2)	3555 (4)	38 (1)	N(*P*2)	3567 (2)	6321 (2)	4081 (3)	35 (1)
C(*A*10)	592 (3)	4417 (2)	2334 (4)	40 (1)	C(*P*11)	2716 (3)	6184 (2)	4301 (4)	42 (1)
C(*A*11)	1321 (2)	286 (2)	961 (3)	33 (1)	C(*P*12)	2113 (3)	6684 (3)	4071 (4)	51 (1)
C(*A*12)	74 (2)	−7 (2)	2030 (3)	32 (1)	C(*P*13)	2400 (3)	7328 (3)	3615 (4)	55 (1)
N(*A*1)	−1167 (2)	4359 (2)	4084 (4)	58 (1)	C(*P*14)	3270 (3)	7445 (2)	3361 (4)	51 (1)
N(*A*2)	957 (3)	4859 (2)	1865 (4)	61 (1)	C(*P*15)	3842 (3)	6937 (2)	3598 (4)	44 (1)
N(*A*3)	1877 (2)	12 (2)	439 (3)	50 (1)	C(*P*16)	4241 (3)	5810 (2)	4410 (4)	44 (1)
N(*A*4)	−349 (2)	−505 (2)	2329 (3)	48 (1)	C(*P*17)	4891 (3)	6247 (2)	5708 (4)	53 (1)
C(*B*1)	1750 (2)	2317 (2)	4962 (3)	28 (1)	C(*P*18)	4464 (3)	6434 (3)	6955 (5)	66 (2)
C(*B*2)	2458 (2)	2032 (2)	4273 (3)	29 (1)	C(*P*19*a*)†	4019 (5)	5705 (4)	7332 (7)	49 (2)
C(*B*3)	2587 (2)	1251 (2)	4022 (3)	29 (1)	C(*P*19*b*)†	4251 (18)	5501 (15)	7436 (27)	78 (10)
C(*B*4)	2005 (2)	678 (2)	4423 (3)	26 (1)	C(*P*19*c*)†	3853 (14)	5914 (9)	7213 (20)	51 (7)
C(*B*5)	1282 (2)	958 (2)	5092 (3)	27 (1)	H(*A*2)	130 (2)	314 (2)	155 (3)	37 (7)
C(*B*6)	1169 (2)	1740 (2)	5348 (3)	29 (1)	H(*A*3)	153 (2)	180 (2)	108 (3)	26 (6)
C(*B*7)	1635 (2)	3119 (2)	5243 (3)	31 (1)	H(*A*5)	−62 (2)	128 (2)	292 (3)	36 (7)
C(*B*8)	2135 (2)	−126 (2)	4176 (3)	29 (1)	H(*A*6)	−81 (2)	262 (2)	342 (3)	33 (7)
C(*B*9)	955 (3)	3423 (2)	5983 (4)	40 (1)	H(*B*2)	283 (2)	241 (2)	401 (3)	33 (7)
C(*B*10)	2193 (2)	3700 (2)	4834 (4)	39 (1)	H(*B*3)	308 (2)	107 (2)	356 (3)	37 (7)
C(*B*11)	2851 (2)	−420 (2)	3524 (3)	33 (1)	H(*B*5)	87 (2)	54 (2)	533 (3)	33 (7)
C(*B*12)	1560 (2)	−716 (2)	4530 (3)	33 (1)	H(*B*6)	69 (2)	190 (2)	575 (3)	25 (6)
N(*B*1)	418 (3)	3662 (2)	6593 (4)	63 (1)	H(*C*2)	435 (2)	157 (2)	660 (3)	24 (6)
N(*B*2)	2635 (2)	4163 (2)	4492 (4)	58 (1)	H(*C*3)	462 (2)	24 (2)	621 (3)	34 (7)
N(*B*3)	3414 (2)	−681 (2)	3010 (3)	50 (1)	H(*C*5)	245 (2)	−30 (2)	791 (3)	34 (7)
N(*B*4)	1114 (2)	−1217 (2)	4789 (4)	50 (1)	H(*C*6)	215 (2)	104 (2)	835 (3)	33 (7)
C(*C*1)	3234 (2)	1461 (2)	7516 (3)	29 (1)	H(*D*2)	598 (2)	89 (2)	−70 (3)	34 (7)
C(*C*2)	3966 (2)	1194 (2)	6870 (3)	30 (1)	H(*D*3)	371 (2)	44 (2)	99 (3)	33 (7)
C(*C*3)	4126 (2)	425 (2)	6657 (3)	31 (1)	H(*P*1)	58 (2)	597 (2)	75 (4)	60 (9)
C(*C*4)	3567 (2)	−160 (2)	7054 (3)	28 (1)	H(*P*2)	4 (3)	727 (2)	159 (4)	68 (10)
C(*C*5)	2821 (2)	99 (2)	7672 (3)	31 (1)	H(*P*3)	73 (2)	837 (2)	118 (4)	61 (9)
C(*C*6)	2660 (2)	870 (2)	7890 (3)	30 (1)	H(*P*4)	202 (3)	843 (3)	2 (4)	85 (12)
C(*C*7)	3073 (2)	2261 (2)	7770 (3)	31 (1)	H(*P*5)	244 (2)	707 (2)	−76 (3)	52 (9)
C(*C*8)	3744 (2)	−952 (2)	6872 (3)	32 (1)	H(*P*6*a*)	196 (2)	566 (2)	−153 (3)	53 (9)
C(*C*9)	2327 (2)	2512 (2)	8389 (3)	35 (1)	H(*P*6*b*)	125 (2)	522 (2)	−82 (4)	59 (9)
C(*C*10)	3636 (2)	2865 (2)	7425 (3)	36 (1)	H(*P*7*a*)	247 (2)	562 (2)	119 (3)	50 (8)
C(*C*11)	4499 (2)	−1221 (2)	6310 (3)	34 (1)	H(*P*7*b*)	312 (2)	596 (2)	39 (3)	51 (9)
C(*CU*1)	3205 (2)	−1538 (2)	7286 (4)	35 (1)	H(*P*8*a*)†	223 (3)	424 (3)	−43 (5)	58 (13)
N(*C*1)	1725 (2)	2708 (2)	8869 (3)	49 (1)	H(*P*8*b*)†	301 (3)	460 (3)	24 (5)	47 (12)
N(*C*2)	4089 (2)	3353 (2)	7149 (4)	53 (1)	H(*P*9*a*)†	384 (4)	397 (4)	27 (7)	46 (16)
N(*C*3)	5099 (2)	−1456 (2)	5864 (3)	50 (1)	H(*P*9*b*)†	396 (4)	486 (4)	125 (7)	45 (16)
N(*C*4)	2776 (2)	−2023 (2)	7606 (4)	53 (1)	H(*P*9*c*)†	324 (4)	435 (4)	143 (7)	46 (16)
C(*D*1)	4837 (2)	803 (2)	146 (3)	30 (1)	H(*P*11)	258 (2)	571 (2)	463 (3)	48 (8)
C(*D*2)	5584 (2)	519 (2)	−446 (3)	33 (1)	H(*P*12)	145 (2)	650 (2)	412 (3)	59 (9)
C(*D*3)	4258 (2)	241 (2)	585 (3)	31 (1)	H(*P*13)	194 (2)	766 (2)	341 (3)	56 (9)
C(*D*4)	4679 (2)	1588 (2)	282 (3)	31 (1)	H(*P*14)	346 (2)	788 (2)	291 (3)	56 (9)
C(*D*5)	3944 (2)	1885 (2)	891 (4)	38 (1)	H(*P*15)	448 (2)	697 (2)	345 (3)	57 (9)
C(*D*6)	5247 (2)	2142 (2)	−161 (3)	37 (1)	H(*P*16*a*)	456 (2)	567 (2)	362 (3)	51 (8)
N(*D*1)	3367 (2)	2130 (2)	1388 (4)	56 (1)	H(*P*16*b*)	388 (2)	529 (2)	446 (3)	49 (8)
N(*D*2)	5703 (2)	2584 (2)	−525 (4)	54 (1)	H(*P*17*a*)	522 (2)	685 (2)	570 (3)	56 (9)
N(*P*1)	1510 (2)	6466 (2)	−48 (3)	39 (1)	H(*P*17*b*)	534 (2)	590 (2)	590 (3)	56 (9)
C(*P*1)	828 (3)	6502 (3)	668 (4)	48 (1)	H(*P*18*a*)	500 (2)	668 (2)	777 (3)	61 (9)
C(*P*2)	533 (3)	7220 (3)	1123 (4)	57 (2)	H(*P*18*b*)	407 (2)	678 (2)	687 (3)	55 (9)
C(*P*3)	942 (3)	7898 (3)	881 (4)	56 (1)	H(*P*19*a*)†	395 (4)	587 (3)	832 (6)	53 (14)
C(*P*4)	1643 (3)	7864 (2)	183 (4)	51 (1)	H(*P*19*b*)†	348 (4)	549 (3)	669 (6)	52 (14)
C(*P*5)	1910 (3)	7134 (2)	−282 (4)	44 (1)	H(*B*19*c*)†	430 (4)	533 (3)	723 (6)	52 (14)

† The populations for disordered atoms are C(*P*8*a*) = H(*P*8*a*) = H(*P*8*b*) = 0·7, C(*P*8*b*) = C(*P*8*c*) = 0·15, C(*P*9*a*) = H(*P*9*a*) = H(*P*9*b*) = H(*P*9*c*) = 0·5, C(*P*9*b*) = C(*P*9*c*) = 0·25, C(*P*19*a*) = H(*P*19*a*) = H(*P*19*b*) = H(*P*19*c*) = 0·6 and C(*P*19*b*) = C(*P*19*c*) = 0·2.

Results and discussion

(i) *NPPy*$^+$.*(TCNQ)*$_2^-$

Packing. Projections of the structure along **a** and **c** are shown in Fig. 1(*a*) and (*b*) respectively. The structure is dominated by segregated columns of TCNQ anions stacked plane-to-plane along **a**. The layers of TCNQ anions are formed parallel to the *ac* plane, separated by layers of $NPPy^+$ cations. The four TCNQ molecules per unit cell form two crystallographically independent dimers [TCNQ(*A*)–(*A'*) and TCNQ(*B*)–(*B'*)] within which the two TCNQ molecules are related centrosymmetrically. This structure is similar to that observed in [1,4-bis(*N*-pyridiniomethyl)benzene]$^{2+}$.$(TCNQ)_4^{2-}$ (Ashwell, Wallwork, Baker & Berthier, 1975) and (1,1'-ethylene-2,2'-bipyridylium)$^{2+}$.$(TCNQ^-)_2$ (Sundaresan & Wallwork, 1972). Interplanar distances between the least-squares planes through the quinodimethane moieties within two dimers are 3·234 and 3·185 Å for TCNQ(*A*)–(*A'*) and TCNQ(*B*)–(*B'*), respectively, the planes within two dimers being parallel to each other by centrosymmetry. On the other hand, the dihedral angle between adjacent TCNQ(*A*) and (*B*) (*i.e.* between two dimers) is 17·5 (3)°. Several short contacts occur between C atoms of $NPPy^+$ cations and N atoms of the terminal $C(CN)_2$ of the TCNQ anions but the very short contacts between N atoms of cations and anions observed in (1,1'-ethylene-2,2'-bipyridylium)$^{2+}$.$(TCNQ^-)_2$ are not present in this case (Table 3). This suggests that the localization of negative charge on a particular TCNQ site does not occur in the $NPPy^+.(TCNQ)_2^-$ complex. The large dihedral angle between the two dimers appears to be due to the interaction between cations and anions. The overlapping modes within two dimers are ring–external-bond type for both, as observed in many TCNQ radical salts. On the other hand, no direct overlap is seen between adjacent dimers, as shown in Fig. 2. The characteristic stacking in this TCNQ radical salt can be clearly illustrated on a projection viewed along **b** (Fig. 3). Comparison of this figure with Fig. 6(*a*), showing a typical stacking mode, indicates that this structure is essentially similar to that in $MEM^+.(TCNQ)_2^-$ (Bosch & van Bodegom, 1977) and $TMPD^+.(TCNQ)_2^-$ (TMPD = tetramethyl-*p*-phenylenediamine) (Hanson, 1968) with respect to the stacking mode in a zigzag way. This stacking is considered to be important for the phase-transition phenomena as will be described later.

Molecular geometries. Table 4 gives the deviations of atoms from the least-squares planes of the TCNQ anions and the $NPPy^+$ cation. The planes of the terminal $C(CN)_2$ groups of TCNQ(*A*) are twisted around the long axis of the molecule. On the other hand, those of TCNQ(*B*) are bowed in a direction away from the centrosymmetrically related TCNQ(*B'*). This results from the repulsion between TCNQ(*B*) and (*B'*) owing to a very short interplanar distance between them; the separation between best planes through their benzenoid rings is 3·160 Å. The boat form is also observed in $Rb^+.TCNQ^-$ (Hoekstra, Spoelder & Vos, 1972), tetraphenylphosphonium–$(TCNQ)_2^-$ (Goldstein, Seff & Trueblood, 1968) and $MEM^+.(TCNQ)_2^-$ which have comparatively short interplanar separations between TCNQ's.

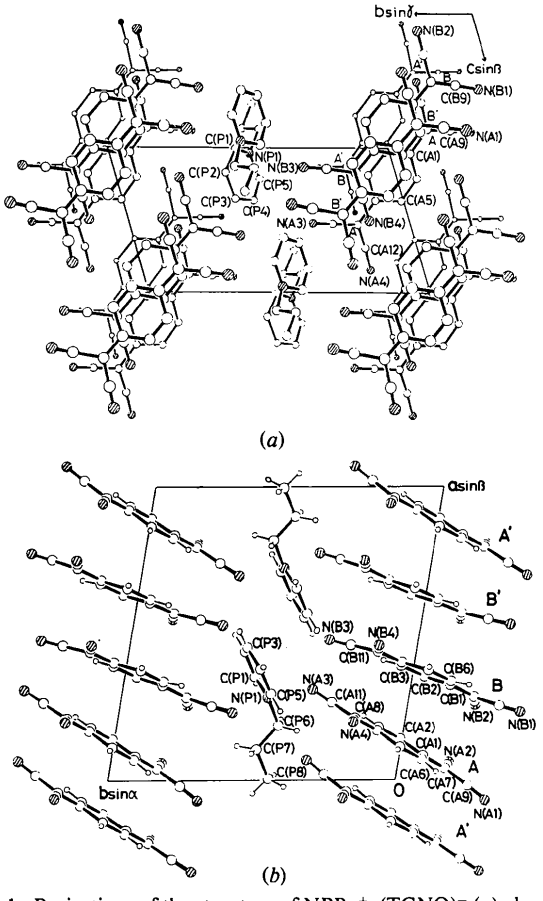

Fig. 1. Projections of the structure of $NPPy^+.(TCNQ)_2^-$ (*a*) along **a** and (*b*) along **c**.

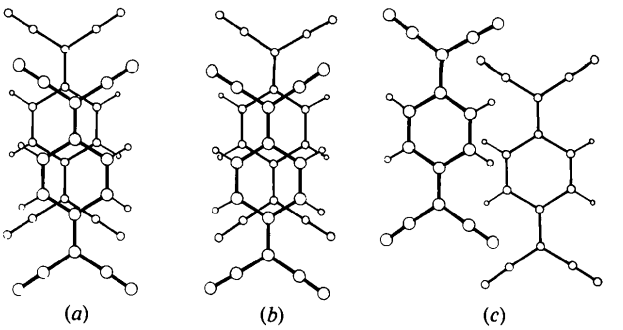

Fig. 2. Nearest-neighbor overlap between (*a*) TCNQ(*A*) and (*A'*), (*b*) TCNQ(*B*) and (*B'*), and (*c*) TCNQ(*A*) and (*B*).

Table 3. *Short intermolecular contacts* (Å) *between columns*

C···C and C···N distances shorter than 3·5 Å and those involving H atoms shorter than 2·9 Å are listed.

Symmetry code

None	x, y, z	(iii)	$1-x, 1-y, -z$
(i)	$-x, -y, -z$	(iv)	$x, y, 1+z$
(ii)	$x, 1+y, z$		

Between $NPPy^+$ and TCNQ columns

C(*P*4)···N(*A*3)	3·383 (5)	C(*P*5)···N(*A*3)	3·404 (5)
C(*P*1)···N(*B*1^{II})	3·369 (5)	C(*P*2)···N(*B*3^{III})	3·411 (6)
H(*P*4)···N(*A*3)	2·79 (3)	H(*P*5)···N(*A*1^{I})	2·62 (3)
H(*P*8*b*)···N(*A*1^{II})	2·70 (4)	H(*P*1)···N(*B*1^{II})	2·52 (3)
H(*P*2)···N(*B*3^{III})	2·62 (4)	N(*A*4)···H(*P*6*b*^{IV})	2·64 (3)
N(*A*3)···H(*P*6*a*^{IV})	2·89 (3)		

Between TCNQ columns

C(*A*1)···N(*B*2^{IV})	3·491 (4)	C(*A*5)···N(*A*2^{IV})	3·336 (5)
C(*A*6)···N(*A*2^{IV})	3·337 (5)	C(*A*12)···C(*B*3^{IV})	3·364 (4)
N(*A*4)···C(*A*2^{IV})	3·292 (5)	N(*A*4)···C(*A*3^{IV})	3·294 (5)
N(*A*4)···C(*B*3^{IV})	3·474 (4)	N(*B*4)···C(*B*3^{IV})	3·406 (5)
N(*A*4)···H(*A*2^{IV})	2·68 (3)	N(*A*4)···H(*A*3^{IV})	2·71 (3)
N(*B*4)···H(*B*3^{IV})	2·73 (3)	H(*A*5)···N(*A*2^{IV})	2·78 (3)
H(*A*6)···N(*A*2^{IV})	2·74 (3)	H(*B*6)···N(*B*2^{IV})	2·83 (3)

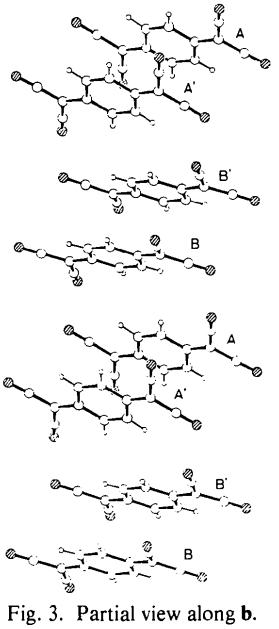

Fig. 3. Partial view along **b**.

The bond lengths and angles in TCNQ(*A*) and (*B*) are given in Fig. 4 and the mean lengths of chemically equivalent bonds are summarized in Table 5. The mean bond lengths of TCNQ(*A*) and (*B*) are identical within their standard deviations. This suggests that unit negative charge is delocalized with $-\frac{1}{2}$ charge on each TCNQ molecule. Two $NPPy^+$ cations are related centrosymmetrically and their pyridine rings are parallel to each other with an interplanar distance of 3·674 Å; no direct overlap occurs. The dimensions of the $NPPy^+$ cation are given in Fig. 5.

Table 4. *Some least-squares planes and deviations* (Å) *of atoms from them*

In each of the equations of the planes, X, Y and Z are coordinates (Å) referred to the orthogonal axes; X along **a**, Y in the *ab* plane and Z along **c***. Atoms marked with daggers were included in the calculations of the least-squares planes.

(*a*) TCNQ(*A*) quinonoid ring

$$0{\cdot}8160X - 0{\cdot}4950Y + 0{\cdot}2987Z = 1{\cdot}6169$$

C(*A*1)†	−0·002 (3)	C(*A*9)	0·041 (4)
C(*A*2)†	−0·008 (3)	C(*A*10)	−0·020 (4)
C(*A*3)†	0·005 (3)	C(*A*11)	0·039 (4)
C(*A*4)†	0·004 (3)	C(*A*12)	−0·051 (4)
C(*A*5)†	−0·005 (3)	N(*A*1)	0·093 (4)
C(*A*6)†	0·001 (3)	N(*A*2)	−0·031 (4)
C(*A*7)†	0·005 (3)	N(*A*3)	0·088 (4)
C(*A*8)†	0·000 (4)	N(*A*4)	−0·105 (4)

(*b*) TCNQ(*B*) quinonoid ring

$$0{\cdot}9520X - 0{\cdot}2545Y + 0{\cdot}1704Z = 5{\cdot}3290$$

C(*B*1)†	−0·002 (9)	C(*B*9)	0·066 (9)
C(*B*2)†	−0·016 (9)	C(*B*10)	0·049 (9)
C(*B*3)†	−0·016 (9)	C(*B*11)	0·124 (9)
C(*B*4)†	−0·002 (9)	C(*B*12)	0·042 (9)
C(*B*5)†	−0·021 (9)	N(*B*1)	0·063 (9)
C(*B*6)†	−0·011 (9)	N(*B*2)	0·049 (9)
C(*B*7)†	0·034 (9)	N(*B*3)	0·207 (9)
C(*B*8)†	0·037 (9)	N(*B*4)	0·053 (9)

(*c*) TCNQ(*B*) benzenoid ring

$$0{\cdot}9519X - 0{\cdot}2553Y + 0{\cdot}1695Z = 5{\cdot}3414$$

C(*B*1)†	0·008 (4)	C(*B*9)	0·073 (5)
C(*B*2)†	−0·006 (4)	C(*B*10)	0·056 (5)
C(*B*3)†	−0·004 (4)	C(*B*11)	0·140 (5)
C(*B*4)†	0·011 (4)	C(*B*12)	0·058 (5)
C(*B*5)†	−0·009 (4)	N(*B*1)	0·069 (5)
C(*B*6)†	0·000 (4)	N(*B*2)	0·055 (5)
C(*B*7)	0·042 (4)	N(*B*3)	0·224 (5)
C(*B*8)	0·052 (4)	N(*B*4)	0·070 (5)

(*d*) $NPPy^+$ pyridinium ring

$$-0{\cdot}6000X + 0{\cdot}7852Y + 0{\cdot}1532Z = 3{\cdot}1416$$

N(*P*1)†	−0·002 (3)	C(*P*5)†	0·003 (4)
C(*P*1)†	−0·002 (4)	C(*P*6)	−0·093 (4)
C(*P*2)†	0·005 (4)	C(*P*7)	−1·487 (4)
C(*P*3)†	−0·003 (4)	C(*P*8)	−1·526 (5)
C(*P*4)†	−0·001 (4)		

Phase transition. Crystal specimens were heated in a stream of electrically heated air. Oscillation photographs along **a** and Weissenberg photographs around **b** were taken for the high-temperature phase. The phase transition began to occur abruptly at about 388 K and it took as long as 30 min to complete, which may indicate that the latent heat is large. The surface of the crystals changed to be rugged (like coal) above the transition temperature and the peak width of all Bragg reflections became diffuse at about 10° in ω. Reflections with h = odd disappeared completely in the

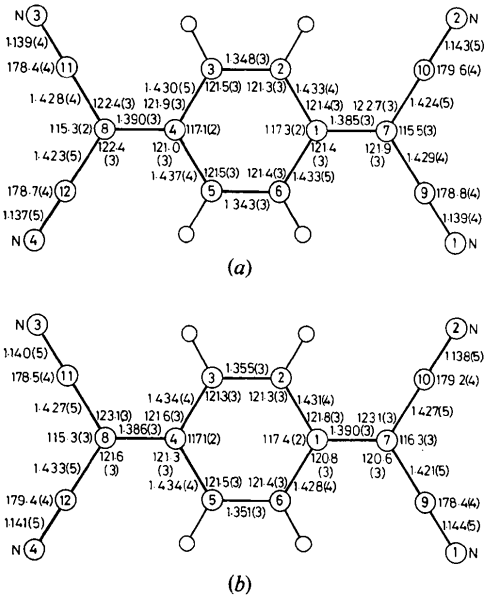

Fig. 4. The bond lengths (Å) and bond angles (°) with their standard deviations in parentheses: (*a*) TCNQ(*A*) and (*b*) TCNQ(*B*).

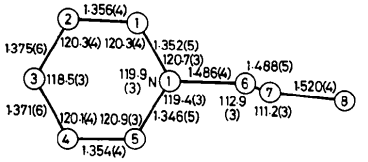

Fig. 5. The bond lengths (Å) and bond angles (°) in the $NPPy^+$ cation.

high-temperature phase. The photographs of the high-temperature phase indicated that the space group remained the same for the high-temperature phase, that *a* became half that of the low-temperature phase. and that *b* and *c* did not change appreciably.

When specimens, heated once above the transition temperature, were cooled again to room temperature, the diffraction pattern of oscillation photographs around **a** differed from that of the high-temperature phase but *a* remained the same as that of the high-temperature form; *i.e.* the specimen changed to a third phase (β form) different from the previous room-temperature phase (α form). This observation is in accord with the result of electrical-conductivity measurements (Murakami & Yoshimura, 1980).

Unit-cell dimensions of the low-temperature phase were determined in the temperature range from 297 to 383 K by least-squares calculations on the basis of 14 to 20 reflections measured on an automated four-circle diffractometer. The temperature variations of the lattice constants are given in Table 6. The unit-cell edge *c* hardly changes, whereas *a* and *b* increase markedly. A large structural change seems to be found along the latter axes over the phase transition. Though the intensity data of the high-temperature phase could not be collected on an automated diffractometer owing to breaking of the crystals, the above observations enabled us to propose a plausible model of the phase transition as follows. There are two TCNQ anions and one $NPPy^+$ cation per unit cell in the high-temperature phase as well as in the β form of the low-temperature phase, whereas there are two cations and four anions in the α form. The halving of *a* affords the following two requirements for the crystal structure above the

Table 5. *Mean bond lengths* (Å) *of the TCNQ molecules in* $NPPy^+.(TCNQ)_2^-$ *and* $(NBPy^+)_4.(TCNQ)_7^{4-}$

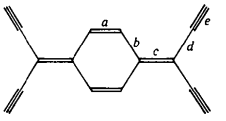

	a	*b*	*c*	*d*	*e*
$NPPy^+.(TCNQ)_2^-$					
TCNQ(*A*)	1·346 (3)	1·433 (4)	1·388 (3)	1·426 (4)	1·140 (4)
TCNQ(*B*)	1·353 (3)	1·432 (4)	1·388 (3)	1·427 (5)	1·141 (5)
$(NBPy^+)_4.(TCNQ)_7^{4-}$					
TCNQ(*A*)	1·353 (5)	1·426 (5)	1·400 (5)	1·424 (5)	1·143 (5)
TCNQ(*B*)	1·351 (5)	1·432 (5)	1·388 (5)	1·426 (5)	1·145 (5)
TCNQ(*C*)	1·353 (5)	1·429 (5)	1·401 (5)	1·423 (5)	1·143 (5)
TCNQ(*D*)	1·342 (5)	1·436 (5)	1·385 (5)	1·428 (5)	1·142 (5)
*$TCNQ^-$	1·360 (11)	1·422 (10)	1·420 (5)	1·418 (7)	1·143 (5)
†$TCNQ^0$	1·344 (4)	1·442 (3)	1·373 (4)	1·435 (3)	1·138 (3)

* Konno & Saito (1973, 1975); Konno, Ishii & Saito (1977).
† Long, Sparks & Trueblood (1965).

Table 6. *Temperature dependence of the lattice constants for* $NPPy^+.(TCNQ)_2^-$

Temperature (K)	a (Å)	b (Å)	c (Å)	α (°)	β (°)	γ (°)	V (Å^3)
297	14·542 (2)	13·723 (2)	7·802 (1)	104·06 (1)	110·72 (2)	94·08 (1)	1391·2 (2)
313	14·560 (4)	13·750 (2)	7·802 (2)	104·09 (2)	110·67 (2)	94·17 (2)	1395·6 (5)
333	14·586 (4)	13·794 (2)	7·805 (2)	104·17 (2)	110·61 (2)	94·38 (2)	1402·0 (5)
353	14·625 (6)	13·856 (4)	7·806 (3)	104·27 (3)	110·51 (4)	94·61 (3)	1411·2 (8)
363	14·636 (8)	13·896 (5)	7·807 (3)	104·39 (3)	110·51 (4)	94·72 (4)	1415·2 (10)
373	14·667 (7)	13·921 (4)	7·803 (3)	104·45 (3)	110·48 (4)	94·82 (3)	1419·2 (8)
383	14·715 (8)	13·974 (5)	7·797 (4)	104·52 (4)	110·50 (4)	95·09 (4)	1425·9 (10)

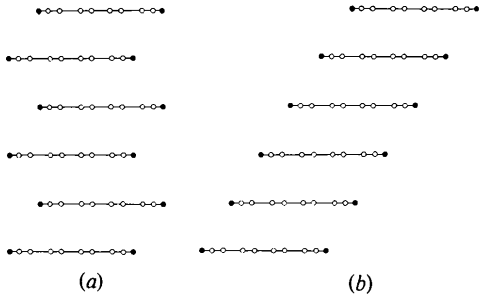

Fig. 6. Typical stacking modes.

transition temperature: Firstly, the two $NPPy^+$ cations related by a center of symmetry in the α form must be congruent by a unit translation along **a**. This may be realized by rotation of the $NPPy^+$ cations or orientational disorder of the cations above the transition temperature. In fact, the entropy of transition suggests such orientational disorder. Murakami & Yoshimura (1980) reported that the increase in the entropy of the transition from the α form to the high-temperature phase is larger by 9·28 J K^{-1} mol^{-1} than that from the β form to the high-temperature phase. The orientational disorder of the $NPPy^+$ cation might contribute to this difference between the α and β forms by $R \ln 2 = 5{\cdot}77$ J K^{-1} mol^{-1}, if the β form and the high-temperature form are assumed to exhibit exact twofold orientational disorder. Secondly, TCNQ(A) and (B') which are crystallographically independent at low temperature must be related by unit translation along **a**. As a result, all the TCNQ's will be parallel to each other. It was reported that the crystal changed from insulator to metal at 383 K on the basis of the measurement of electrical conductivity (Murakami & Yoshimura, 1980). This suggests that a uniform stack of TCNQ's will be formed above the transition temperature. The TCNQ moiety appears to be able to rotate easily around the long axis of the molecule without suffering from any large steric hindrance so that it may stack uniformly above the transition temperature with the overlapping mode of ring–external-bond type as shown in Fig. 6(a), thus manifesting metallic nature.

Materials which undergo a phase transition among quasi-one-dimensional TCNQ salts with charge density $\rho = \frac{1}{2}$ are classified into two types. One type involves crystals of quinolinium–$(TCNQ)_2$, acridinium–$(TCNQ)_2$ and tetrathiatetracene–$(TCNQ)_2$. They undergo a gradual phase transition without a clear transition temperature (Buravov, Fedutin & Shchegolev, 1971; Shchegolev, 1972; Buravov, Fremenko, Lyubovskii, Rozenberg, Khidekel, Shibaeva, Shchegolev & Yagubskii, 1974). Their columnar structures of the TCNQ anions have a uniform stack as shown in Fig. 6(b) (Kobayashi, Marumo & Saito, 1971; Kobayashi, 1974; Shibaeva & Rozenberg, 1976). The other type includes crystals of NPPy–$(TCNQ)_2$, MEM–$(TCNQ)_2$ and TMPD–$(TCNQ)_2$. The first two undergo a first-order phase transition changing from metal to insulator accompanying a lattice distortion with wavevector $4\mathbf{k}_F$ (Coll, 1974; Bernasconi, Rice, Schneider & Strässler, 1975; Emery, 1976; Torrance, 1977). In the MEM–TCNQ salt, a spin Peierls phase transition with a lattice distortion of $2\mathbf{k}_F$ was observed at 20 K. The columnar structure in the high-temperature phase of these crystals involves an almost regular stacking with overlapping mode similar to that in the first type but in a zigzag way (Fig. 6a) (Huizinga, Kommandeur, Sawatzky, Thole, Kopinga, de Jonge & Roos, 1979).

It was reported that the crystal of TMPD–$(TCNQ)_2$ has a uniform columnar structure (Hanson, 1968) but is non-metallic at room temperature (Somoano, Hadek, Yen & Rembaum, 1975). However, this crystal might become metallic above 300 K, judging from the observation that the electrical resistivity levels off in the region 300–340 K and increases irreversibly with a further rise of temperature.

Sumi (1977) reported that quasi-one-dimensional TCNQ radical salts have strong electron–electron correlation and that the fluctuation with wavevector $4\mathbf{k}_F$ is stronger than that of $2\mathbf{k}_F$ in the strong electron–lattice interaction system. Structure (a) with a zigzag chain appears to have a stronger electron–lattice interaction than the structure (b) due to the instability for the phonon mode of dimerization.

(ii) $(NBPy^+)_4.(TCNQ)_7^{4-}$

Projections of the structure along **b** and **c** are shown in Fig. 7(a) and (b). The TCNQ molecules are stacked plane-to-plane along [102] and form a heptamer in

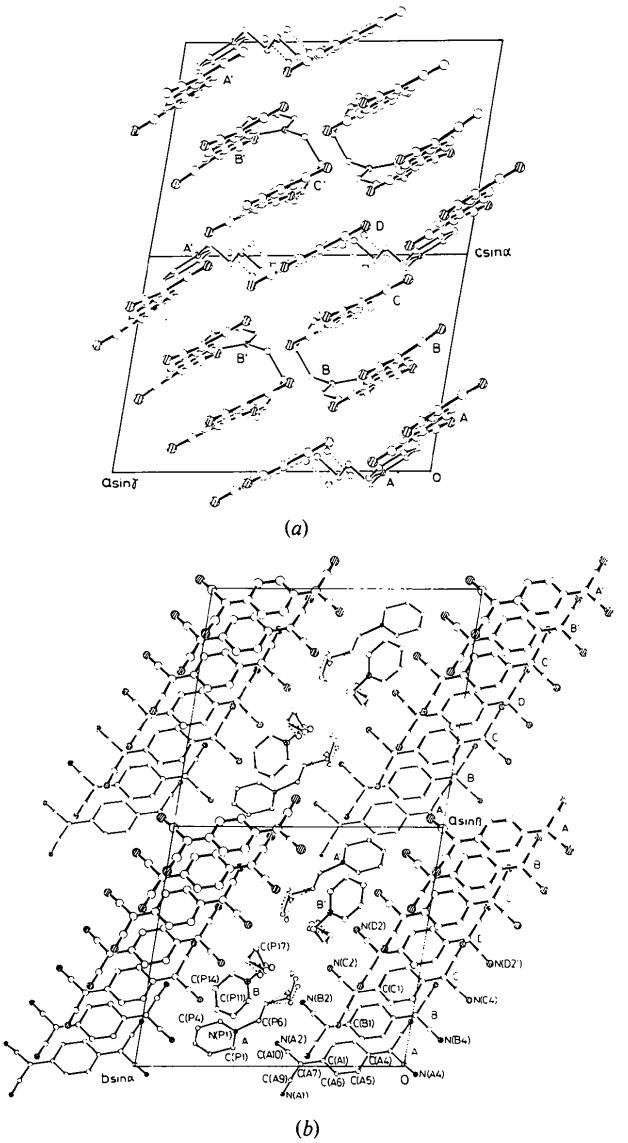

Fig. 7. Projections of the structure of $(NBPy^+)_4.(TCNQ)_7^{4-}$ (*a*) along **b** and (*b*) along **c**. Disordered butyl groups of $NBPy^+$ cations are illustrated by broken lines.

which four electrons are distributed. Monomer, dimer, trimer, tetramer and pentamer forms of TCNQ have hitherto been reported. TCNQ(*D*) is positioned on a symmetry center. The interplanar distances of the best planes through quinodimethane moieties between TCNQ(*A*)–(*B*), (*B*)–(*C*) and (*C*)–(*D*) are 3·220, 3·329 and 3·363 Å, respectively, and their overlapping modes are ring–external-bond type, similar to that observed in $NPPy^+.(TCNQ)_2^-$. There is slight overlap of terminal $C(CN)_2$ groups between TCNQ(*A*) and (*A'*), *i.e.* between heptamers, with an interplanar distance of 3·340 Å. In the two external bonds of TCNQ(*A*), one overlaps on TCNQ(*B*) and the other on the pyridinium ring of the $NBPy^+(A')$ cation. TCNQ(*A*) and

Table 7. *Short intermolecular contacts* (Å) *between $NBPy^+$ cations and TCNQ anions*

Symmetry code

None	x, y, z	(iii)	$-x, 1-y, -z$
(i)	$x, 1+y, z$	(iv)	$-x, 1-y, 1-z$
(ii)	$1-x, 1-y, 1-z$		

$C(P1)\cdots N(A2)$	3·425 (6)	$C(P7)\cdots N(A2)$	3·411 (6)
$C(P12)\cdots N(A2)$	3·468 (5)	$C(P13)\cdots N(B4^{I})$	3·437 (6)
$C(P14)\cdots N(B3^{I})$	3·356 (6)	$C(P14)\cdots C(C11^{I})$	3·442 (4)
$C(P14)\cdots N(C3^{I})$	3·481 (5)	$C(P15)\cdots N(C3^{I})$	3·304 (4)
$C(P15)\cdots N(C2^{II})$	3·376 (5)	$N(P1)\cdots C(A7^{III})$	3·394 (4)
$C(P1)\cdots C(A10^{III})$	3·406 (5)	$C(P4)\cdots C(A6^{III})$	3·460 (5)
$C(P2)\cdots N(C1^{IV})$	3·415 (5)	$C(P11)\cdots N(A1^{IV})$	3·256 (6)
$C(P12)\cdots N(A1^{IV})$	3·325 (6)		

Table 8. *Bond lengths* (Å) *for two $NBPy^+$ cations*

N(P1)–C(P1)	1·349 (5)	N(P2)–C(P11)	1·336 (5)
N(P1)–C(P5)	1·339 (5)	N(P2)–C(P15)	1·345 (5)
N(P1)–C(P6)	1·495 (5)	N(P2)–C(P16)	1·490 (5)
C(P1)–C(P2)	1·362 (6)	C(P11)–C(P12)	1·370 (6)
C(P2)–C(P3)	1·364 (7)	C(P12)–C(P13)	1·376 (7)
C(P3)–C(P4)	1·362 (7)	C(P13)–C(P14)	1·373 (6)
C(P4)–C(P5)	1·360 (6)	C(P14)–C(P15)	1·350 (6)
C(P6)–C(P7)	1·500 (6)	C(P16)–C(P17)	1·508 (5)
C(P7)–C(P8a)	1·523 (6)	C(P17)–C(P18)	1·509 (7)
C(P8a)–C(P9a)	1·523 (9)	C(P18)–C(P19a)	1·531 (9)

$NBPy^+(A')$ are almost parallel to each other with an interplanar distance of 3·434 Å. Short contacts between $NBPy^+$ cations and TCNQ anions are given in Table 7. The butyl groups of two crystallographically independent $NBPy^+$ cations occupy three different positions with ratios of about 0·7:0·15:0·15 and 0·6:0·2:0·2 for $NBPy^+(A)$ and (*B*) respectively. This orientational disorder in the configuration of the cations seems to suggest that cations may play a main role in the transition where electrical resistivity increases toward the high-temperature phase.

Mean bond lengths of chemically equivalent bonds of TCNQ molecules are given in Table 5. These dimensions indicate intermediate values between $TCNQ^0$ and $TCNQ^{1-}$. There is a tendency for TCNQ(*A*) and (*C*) to carry more negative charge than TCNQ(*B*) and (*D*), judging from their dimensions and particularly from bond lengths *b* and *c* (Table 5) which have been suggested to be more sensitive to the extent of charge (Ashwell, Eley, Drew, Wallwork & Willis, 1978; Wilson, Corvan, Seiders, Hodgson, Brookhart, Hatfield, Miller, Reis, Rogan, Gebert & Epstein, 1979). As the $NBPy^+$ cation has a short contact with TCNQ(*A*), more charge localizes on TCNQ(*A*) owing to the Coulombic attraction between them. More negative charge is distributed on alternate TCNQ sites (*A*), (*C*), (*C'*) and (*A'*) within the heptamer owing to electron–electron repulsion. The dimensions of the $NBPy^+$ cations are given in Table 8.

References

ASHWELL, G. J., ELEY, D. D., DREW, N. J., WALLWORK, S. C. & WILLIS, M. R. (1978). *Acta Cryst.* B**34**, 3608–3612.

ASHWELL, G. J., WALLWORK, S. C., BAKER, S. R. & BERTHIER, P. I. C. (1975). *Acta Cryst.* B**31**, 1174–1178.

BENI, G. & PINCUS, P. (1972). *J. Chem. Phys.* **57**, 3531–3534.

BERNASCONI, J., RICE, M. J., SCHNEIDER, W. R. & STRÄSSLER, S. (1975). *Phys. Rev. B*, **12**, 1090–1092.

BOSCH, A. & VAN BODEGOM, B. (1977). *Acta Cryst.* B**33**, 3013–3021.

BURAVOV, L. I., FEDUTIN, D. N. & SHCHEGOLEV, I. F. (1971). *Sov. Phys. JETP*, **32**, 612–616.

BURAVOV, L. I., FREMENKO, O. N., LYUBOVSKII, R. B., ROZENBERG, L. P., KHIDEKEL, M. L., SHIBAEVA, R. P., SHCHEGOLEV, I. F. & YAGUBSKII, E. B. (1974). *JETP Lett.* **20**, 208–209.

COLL, C. F. (1974). *Phys. Rev. B*, **9**, 2150–2158.

EMERY, V. J. (1976). *Phys. Rev. Lett.* **37**, 107–110.

FLETCHER, J. R. & TOOMBS, G. A. (1977). *Solid State Commun.* **22**, 555–556.

GOLDSTEIN, P., SEFF, K. & TRUEBLOOD, K. N. (1968). *Acta Cryst.* B**24**, 778–791.

HANSON, A. W. (1968). *Acta Cryst.* B**24**, 768–778.

HOEKSTRA, A., SPOELDER, T. & VOS, A. (1972). *Acta Cryst.* B**28**, 14–25.

HUIZINGA, S., KOMMANDEUR, J., SAWATZKY, G. A., THOLE, B. T., KOPINGA, K., DE JONGE, W. J. M. & ROOS, J. (1979). *Phys. Rev. B*, **19**, 4723–4732.

International Tables for X-ray Crystallography (1974). Vol. IV. Birmingham: Kynoch Press.

JACOBS, I. S., BRAY, J. W., HART, H. R. JR, INTERRANTE, L. V., KASPER, J. S., WATKINS, G. D., PROBER, D. E. & BONNER, J. C. (1976). *Phys. Rev. B*, **14**, 3036–3051.

KEPLER, R. G. (1963). *J. Chem. Phys.* **39**, 3528–3532.

KOBAYASHI, H. (1974). *Bull. Chem. Soc. Jpn*, **47**, 1346–1352.

KOBAYASHI, H., MARUMO, F. & SAITO, Y. (1971). *Acta Cryst.* B**27**, 373–378.

KOMMANDEUR, J. (1975). *Low-Dimensional Cooperative Phenomena*, edited by H. J. KELLER. New York: Plenum.

KONNO, M., ISHII, T. & SAITO, Y. (1977). *Acta Cryst.* B**33**, 763–770.

KONNO, M. & SAITO, Y. (1973). *Acta Cryst.* B**29**, 2815–2824.

KONNO, M. & SAITO, Y. (1975). *Acta Cryst.* B**31**, 2007–2012.

LONG, R. E., SPARKS, R. A. & TRUEBLOOD, K. N. (1965). *Acta Cryst.* **18**, 932–939.

MURAKAMI, M. & YOSHIMURA, S. (1980). *Bull. Chem. Soc. Jpn*, **53**, 3504–3509.

PYTTE, E. (1974). *Phys. Rev. B*, **10**, 4637–4642.

SHCHEGOLEV, I. F. (1972). *Phys. Status Solidi A*, **12**, 9–45.

SHIBAEVA, R. P. & ROZENBERG, L. P. (1976). *Sov. Phys. Crystallogr.* **20**, 581–584.

SOMOANO, R., HADEK, V., YEN, S. P. S. & REMBAUM, A. (1975). *J. Chem. Phys.* **62**, 1061–1067.

STEWART, R. F., DAVIDSON, E. R. & SIMPSON, W. T. (1965). *J. Chem. Phys.* **42**, 3175–3187.

SUMI, H. (1977). *Solid State Commun.* **21**, 17–20.

SUNDARESAN, T. & WALLWORK, S. C. (1972). *Acta Cryst.* B**28**, 3065–3074.

TORRANCE, J. B. (1977). *Chemistry and Physics of One-Dimensional Metals*, edited by H. J. KELLER. New York: Plenum.

TORRANCE, J. B. (1978). *Ann. NY Acad. Sci.* **313**, 210–233.

VEGTER, J. G., HIMBA, T. & KOMMANDEUR, J. (1969). *Chem. Phys. Lett.* **3**, 427–429.

WILSON, S. R., CORVAN, P. J., SEIDERS, R. P., HODGSON, D. J., BROOKHART, M., HATFIELD, W. E., MILLER, J. S., REIS, A. H. JR, ROGAN, P. K., GEBERT, E. & EPSTEIN A. J. (1979). *Molecular Metals*, edited by W. E. HATFIELD. New York: Plenum.

YOSHIMURA, S. & MURAKAMI, M. (1978). *Ann. NY Acad. Sci.* **313**, 269–292.

Acta Cryst. (1981). B**37**, 2043–2048

Über die Kristallstruktur und die Absolute Konfiguration des (+)-Chelidonin-*p*-brombenzoats

VON NARAO TAKAO,* NORIKO MORITA, MIYOKO KAMIGAUCHI UND KINUKO IWASA

Pharmazeutische Hochschule für Frauen zu Kobe, Motoyamakitamachi, Higashinada-ku, Kobe 658, *Japan*

UND KEN-ICHI TOMITA, TAKAJI FUJIWARA UND SATOSHI FUJII

Pharmazeutische Fakultät der Universität Osaka, Yamada-kami, Suita, Osaka 565, *Japan*

(*Eingegangen am* 12. *Mai* 1980; *angenommen am* 6. *April* 1981)

Abstract

The crystal structure and absolute configuration of (+)-chelidonine *p*-bromobenzoate ($C_{27}H_{22}BrNO_6$, M_r = 536·36) has been determined. The compound crystallizes in the triclinic space group $P\bar{1}$ with a = 14·257 (5), b = 9·656 (4), c = 10·218 (5) Å, α = 116·90 (3), β = 111·27 (3), γ = 88·27 (2)°, V = 1153·8 Å^3, $F(000)$ = 548, D_m = 1·537, D_x = 1·544

* Korrespondenz bitte an diesen Autor richten.

0567-7408/81/112043-06$01.00